The 2012 World Congress on
Advances in Civil, Environmental, and Materials Research (ACEM' 12)
Seoul, Korea, August 26-30, 2012

Strain Localization in Shear band

*Xu Li[1] and Yang Hui[2]

[1), 2)] *School of Civil Engineering, Beijing JiaoTong University, 100044, Beijing*
[1)] ceXuLi2012@gmail.com

ABSTRACT

Shear band is often formed in tri-axial and bi-axial test. The local strain, stress, and soil properties in shear band determine the soil strength, whereas distinguish with that of whole sample. In this study, bi-axial test is carried out utilizing finite element method (FEM) together with Remeshing and Interpolating Technique with Small Strain (RITSS) method. The results demonstrate that the soil in the shear band yields and dilates gradually. The friction angle decreases continuously until the soil reaches the critical state, as well as the dilatancy angle. The strain localization will not change the soil strength, but do change the apparent stress-strain relation of whole soil sample. Once a "central" shear band of soil at critical state is formed, the apparent shear strength of whole sample reaches the critical value. However the volume of whole sample still increases with yielding of soil in marginal shear band. The apparent axial strain is much smaller than the local one and depends on the sample dimension, and as well as the mesh density to a certain extent.

INTRODUCTION

Soil failure is always happening in local places and expands to the global body. For example, narrow intensive shearing zones, which are normal called as shear bands, are often observed in triaxial or bi-axial test of granular materials (Richard et al. 1996; Alshibli et al. 2003). Much concern has been paid to formation mechanism of shear band, as well as the thickness and inclination of shear band. Experimental evidence proves that single or multiple shear bands is easily formed in bi-axial test, in which new observation methodologies including X-ray are used to observe the evolution of shear bands.

The formation of shear band can definitely determine the global response of soil body and the apparent global response is the basis of the majority constitutive models. However, the deference and connection between the local behavior and the global response is still not clear. To address this problem, bi-axial test is carried out utilizing finite element method (FEM) in this study.

[1)] Associate Professor
[2)] Graduate Student

Methodology

In this study, bi-axial test is carried out utilizing FEM method together with the Remeshing and Interpolating Technique with Small Strain method (RITSS, Hu and Randolph 1998). With RITSS method, the gradually deformed soil body is re-characterized by FEM mesh after a certain steps.

In the simulation, sample was of 200 mm in height and 100 mm in width. Sample was loaded from both ends with a displacement step of 0.0001mm. The sample shape was updated and remeshed every 100 steps. Any element needed to be refined in the following step if the principle strain reached 05%. Constant confining pressure p0 was applied to both sides of the sample. Two boundary conditions were considered: (1) Fully rough boundary: four corner points were restrained in horizontal direction, which is close to the bi-axial test in reality; (2) Fully smooth boundary: only the left bottom corner was fixed in horizontal direction, and all other points on both ends were free to move horizontally.

For comparison with experimental data, soil properties are taken as that of Ottawa sand (Alshibli et al. 2003). In the simulation, Mohr-Coulomb model and critical state Mohr-Coulomb model are used to describe the sand behavior. The critical state Mohr-Coulomb (CSMC) can be used to consider the evolution of friction angle and dilatancy angle with void ratio for sand, by using:

$$\tan\phi = \tan\phi_c + \tan\psi \tag{1}$$

$$\tan\psi \approx A(1-\exp^{sign(\gamma)m|\gamma|^n}) \tag{2}$$

where γ is the soil state parameter and defined as (Been and Jefferies 1985):

$$\gamma = e - e_c \tag{3}$$

And

$$e_c = e_\Gamma - \lambda(\frac{p'}{p_a})^\xi \tag{4}$$

The details introduction to CSMC can be found in Li et al. (2013).

Result and Discussion

The model parameters is calibrated by single element test for Ottawa sand (Alshibli et al. 2003) and further used in the bi-axial test. The close match of the model prediction to the experimental data for single element triaxial test provides a set of model parameters as A = 0.36, m = 8, n = 0.75 (Fig. 1).

When the calibrated parameters were applied to the bi-axial element test conditions, a much lower peak is observed (Fig. 2). However, if the dilatancy angle is increased, as the parameter A in equation 2 was increased from 0.36 to 0.6, the CSMC model shows a similar peak as the experimental data (Fig. 3). Bolton (1986) has also suggested that the dilatancy angle in plane strain test is about 1.6 times of that in triaxial test. This can be justified that different parameters might be needed for triaxial and biaxial test conditions. In the bi-axial test, the post-peak shear behaviors are captured very well.

Fig. 4 depicts the shear band formed in biaxial tests when CSMC model was employed. Single shear band is formed first at 2% axial-strain. Double shear band forms at about 3% axial-strain and evolves gradually. This phenomenon is consist with the observation in Alshibli et al. (2003), in which single shear band is clearly observed at about 10% axial-strain and cross double shear band is clearly observed at about 20% axial-strain.

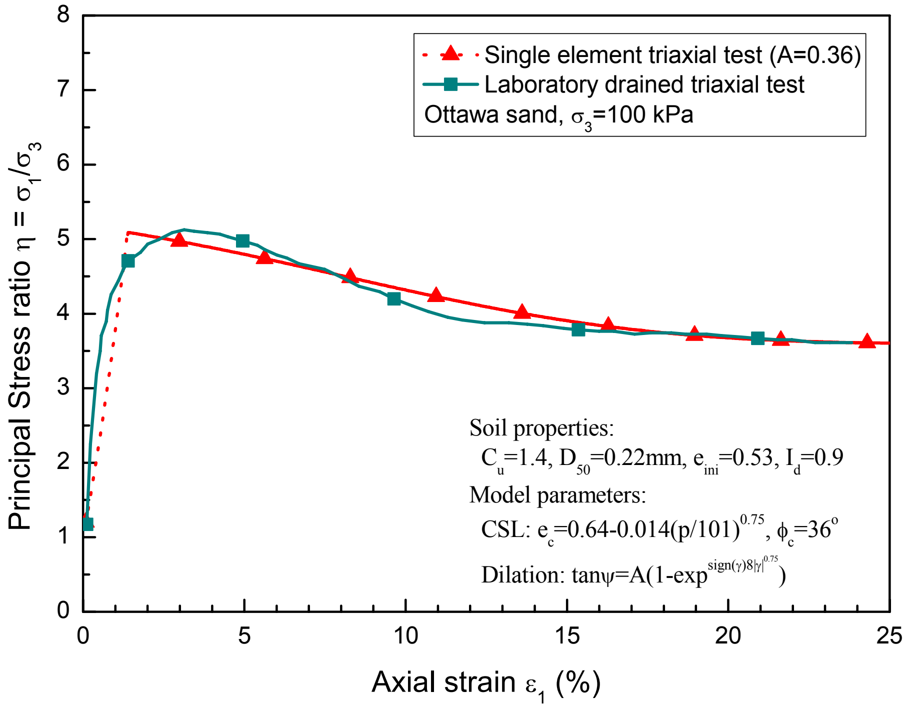

Fig. 1 Model parameter calibration by single element tri-axial test

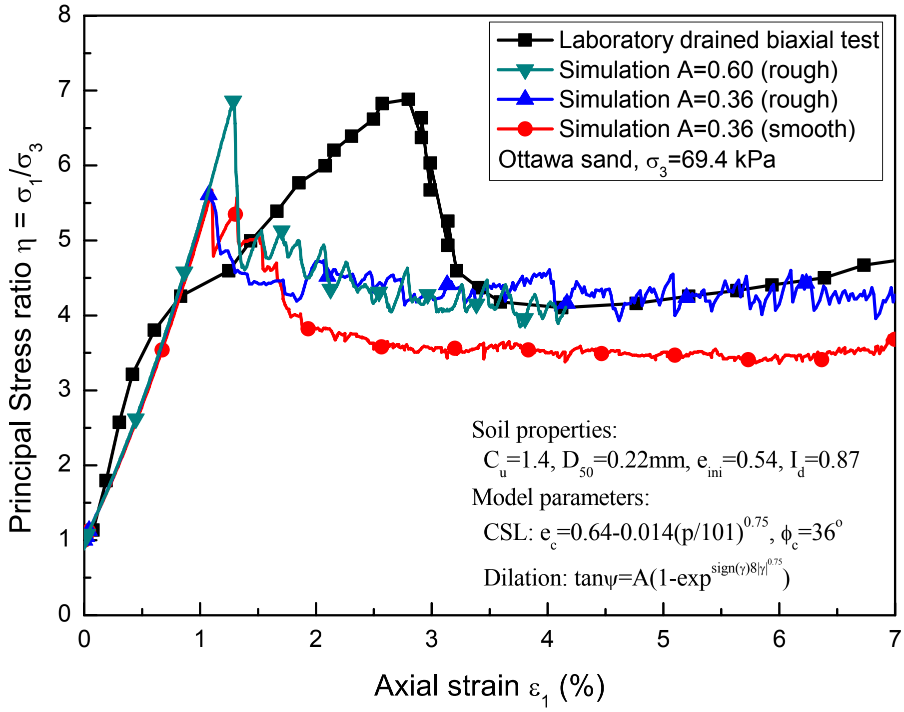

Fig. 2 Bi-axial test result of Ottawa sand simulated by FEM

The soil in the shear band yields and dilates gradually. The void ratio of soil in shear band increases gradually and approaches to the critical void ratio 0.61. The dilatancy angle decreases continuously until the soil reaches the critical state, as well as the friction angle. However, the soil outside the shear band remains the initial void ratio, i.e. 0.54. That's to say, the local strain in shear band is much different with that of whole sample. The local strain, which can be captured by single element test under bi-axial loading condition, is much higher (as shown in Fig. 3). The single element test result shows a slow decrease in the principal stress ratio after its peak than that in biaxial test. In fact, the measured axial strain in laboratory should be an apparent value.

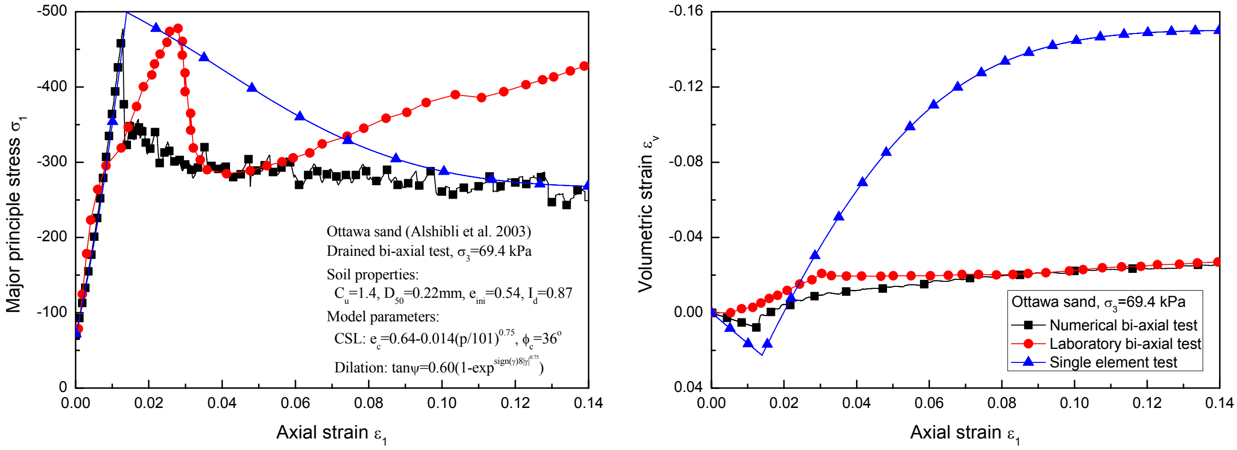

Fig.3 Plane strain experiments of Ottawa sand (fully rough boundary condition): (a) σ_1-ε_1 relation; (b) ε_v-ε_1 relation.

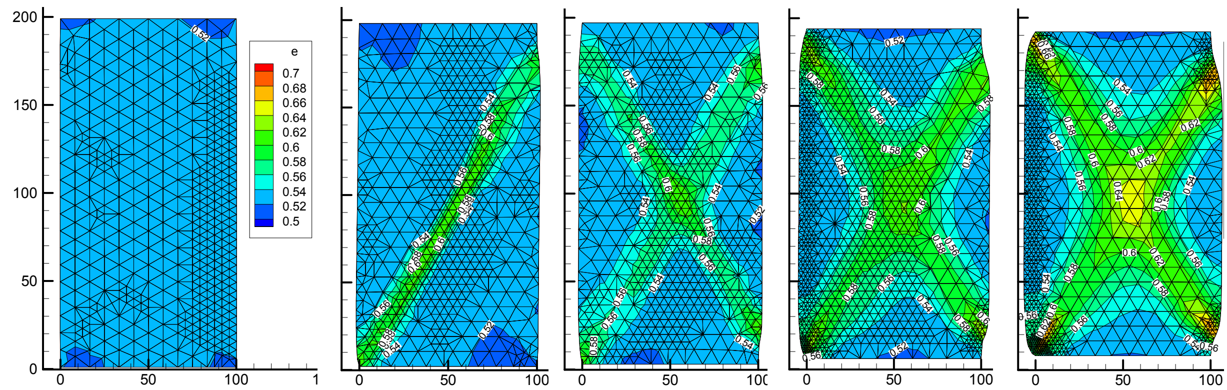

Fig.4 Void ratio field in PS test (fully rough condition):
(a) 1% strain; (b) 2% strain; (c) 3% strain; (d) 6% strain; (e) 9% strain.

It is obvious that the local strain in shear strain is different with the apparent strain of whole sample. The numerical single element test (e.g. Figs. 1 & 3) was conducted on one material point, thus local shear behavior was captured. The biaxial test was conducted on a soil sample, thus an apparent axial strain was obtained. The apparent axial strain is much smaller than the local one and depends on the sample dimension, and as well as the mesh density to a certain extent. Therefore, the single element test result (Figs. 1 & 3) shows a slow decrease in the principal stress ratio after its peak than that in biaxial test (Figs. 2 & 3). The residual strength of soil is approached at 20% of axial strain in Fig. 1 and at 2% of axial strain in Fig. 2.

Strain localization is critical in explaining some laboratory test results where after the peak, the deviatoric stress q often decreases to a stable value much earlier for axial strain than that does for volume strain (Samieh and Wong 1997; Salgado et al. 2000; Alshibli et al. 2003). In Alshibli et al. (2003), the stress start to flocculates around that value after 10% axial strain, otherwise the volume strain continuously increases even over 25% axial strain. Once a "central" shear band of soil at critical state is formed, the apparent shear strength of whole sample reaches the critical value. However the volume of whole sample still increases with yielding of soil in marginal shear band (Figs. 3 & 4).

Under the fully smooth condition, only single shear band is formed as shown in Fig. 5. The friction angle in the shear band is also gradually approach to the critical friction angle 36°. The the orientation of the shear band is changing during loading. This change is displayed in Fig. 6 as the slope of the shear band is shown by vertical displacement contours. Upon loading, the slope is founded to increase from 51° to 62° from the horizontal. The final slope is close to the theoretical value $45 + \phi_c/2 = 45 + 36/2 = 63°$. This change of shear band orientation was also observed in the experiments by Richard et al. (1996), where masonry sand, clean quartz sand with D_{50} of 0.32 mm, was tested and shear band slope varied from 55 to 59°. For the Ottawa sand analyzed here, Alshibli et al. (2003) observed the shear band slope of 53~57°. They didn't mention the change of the shear band orientation during loading.

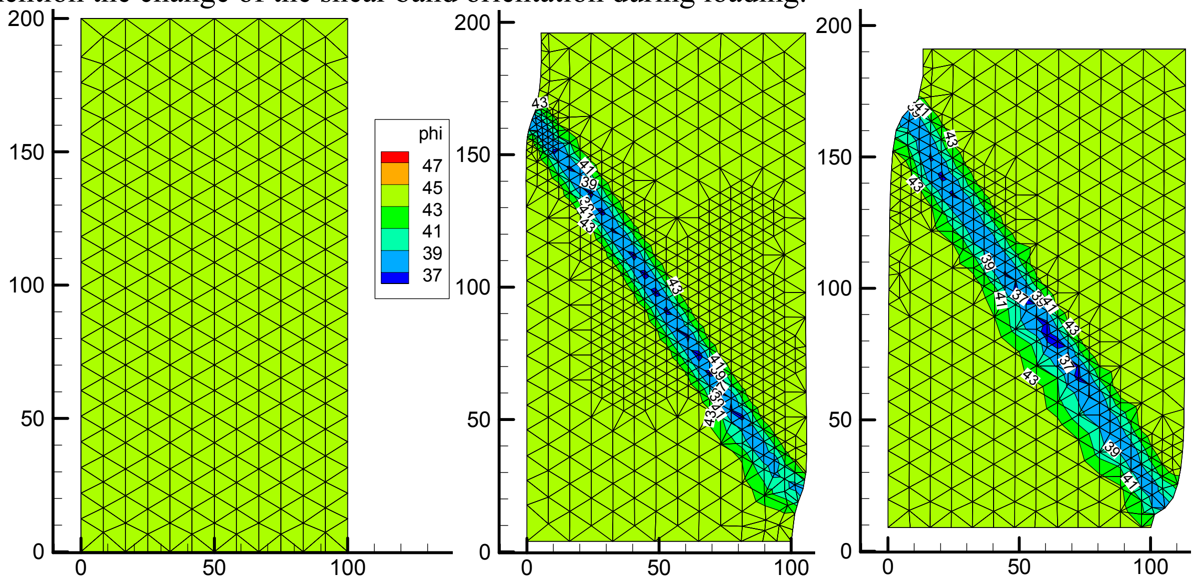

Fig. 5 State dependent friction angles in shear band under smooth boundary condition: (a) initial state; (b) at 4% axial-strain; (c) at 9% axial-strain.

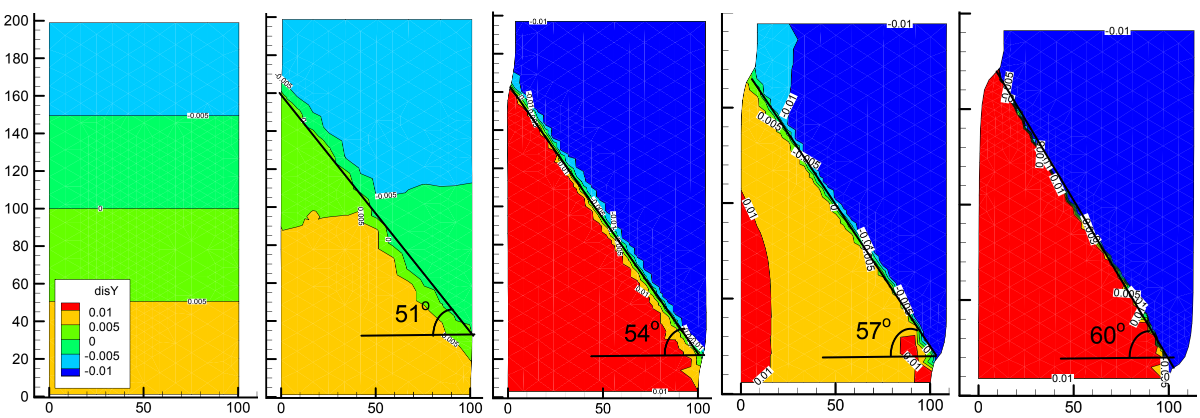

(a) ε_1=1% (b) ε_1=1.2% (c) ε_1=3% (d) ε_1=6% (e) ε_1=9%

Fig. 6 Development of shear band in numerical biaxial test using CSMC model with smooth boundary

The results of CSMC and MC are compared in Fig. 7. CSMC model's prediction can capture the peak strength of sand. With the evolution of shear band, the friction angle in shear band decrease to the critical friction angle, resulting in the residual strength which is matching with prediction of simple MC model.

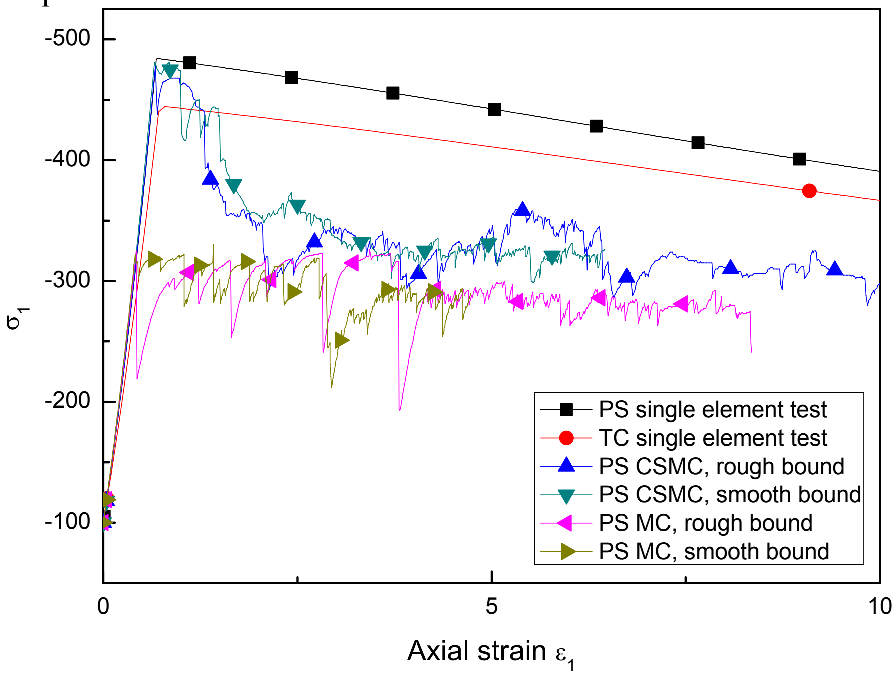

Fig. 7 Shear Strength of sand with CSMC model

The geometry of soil specimen can definitely affect the shearing behavior of sand. The simulation result with different sample geometry is shown in Fig. 8. The σ_1-ε_1 relation is nearly identical in two cases. However, the ε_v-ε_1 relation is dependent on the geometry of soil specimen and the shape of shear band formed.

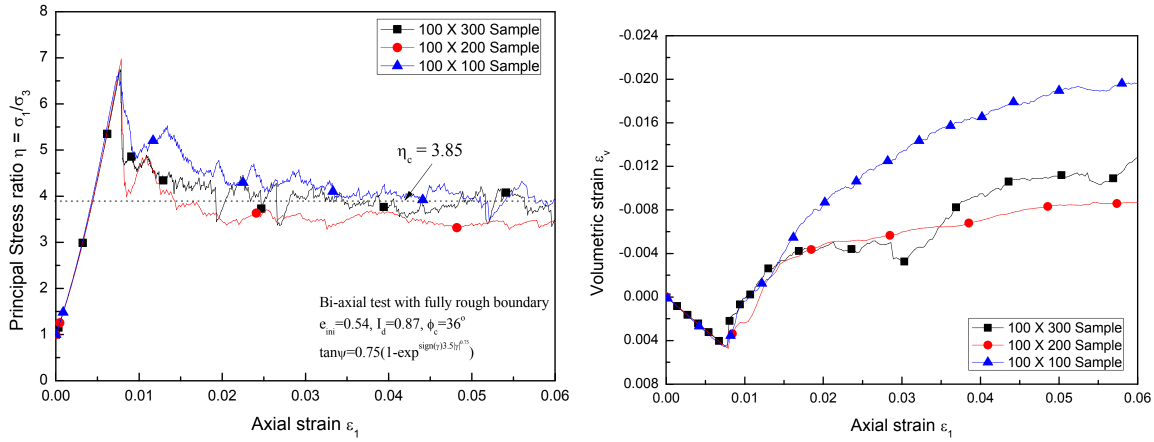

Fig. 8 Effect of geometry on shearing behaviour: (a) σ_1-ε_1 relation; (b) ε_v-ε_1 relation.

CONCLUSION

In this study, the shear band in PS test is studied by FEM method. The simulation results demonstrate that cross shear band is common in PS shearing of sand. The properties of sand in shear band, including void ratio, friction angle and dilatancy angle etc., is of much difference with that out of shear band. The presence of shear band may not cause much difference in the local shear strength and global apparent shear strength, but it true cause significant difference in the local stress-strain relation and the global apparent stress-strain relation. The later part is dependent on the geometry of soil body whereas the front part is not and just controlled by the constitutive model used. Other hints of this study include that FEM with RITSS is an effective method to study the evolution of shear band and CSMC model can catch the peak resistance and ultimate resistance of sand.

Acknowledgement
This study is supported by the Open Funds Projects from Key Laboratory for River Dynamics and Hydraulic Engineering, Tsinghua University (sklhse-2011-D-01).

REFERENCES

Alshibli, K.A. Batiste, S.N. and Sture S. 2003. Strain localization in sand: plane strain versus triaxial compression. Journal of Geotechnical and Geoenvironmental Engineering, 129(6): 483-494.

Bolton, M.D. 1986. The strength and dilatancy of sands. Geotechnique, 36(1): 65-78.

Hu, Y.X. and Randolph, M.F. 1998. H-adaptive FE analysis of elasto-plastic non-homogeneous soil with large deformation. Computers and Geotechnics, 23(1-2): 61-83.

Li X. Hu, Y.X. and White, D. 2013. Development of critical state hyperbolic Mohr-Coulomb model for sand in large deformation FE analysis. Submitted to Geotechnique.

Richard F., Wendell, H., Michael, M. and Gioacchino, V. Strain localization and undrained steady state of sand. Journal of Geotechnical Engineering, 122(6): 462-473.

Samieh, A.M. and R.C.K. Wong. 1997. Deformation of Athabasca oil sand in triaxial compression tests at low effective stresses under varying boundary conditions. Canadian Geotechnical Journal, 34: 985-990.

Salgado R., Bandini, P. and Karim, A. 2000. Shear strength and stiffness of slity sand. Journal of Geotechnical and Geoenvironmental Engineering, 126: 451-461.